Impulsive Noise Cancellation Based on Soft Decision and Recursion

Sina Zahedpour, Soheil Feizi, Arash Amini, Mahmoud Ferdosizadeh, and Farokh Marvasti

***Abstract*—In this paper, we propose a new method to recover band-limited signals corrupted by impulsive noise. The proposed method successively uses adaptive thresholding and soft decisioning to find the locations and amplitudes of the impulses. In our proposed method, after estimating the positions and amplitudes of the additive impulsive noise, an adaptive algorithm, followed by soft decision, is employed to detect and attenuate the impulses. In the next step, by using an iterative method, an approximation of the signal is obtained. This signal approximation is successively used to improve the noise estimate. The algorithm is analyzed and verified by computer simulations. Simulation results confirm the robustness of the proposed algorithm, even if the impulsive noise exceeds the theoretical reconstruction capacity.**

***Index Terms*—Adaptive systems, error correction, impulse noise, recursive estimation, soft decision.**

I. Introduction

IMPULSIVE noise is a common phenomenon that occurs in channels that suffer from switching, manual interruptions, ignition noise, and lightning. Examples of these channels include power-line channels [1], digital-subscriber-line systems [2], and digital TV (e.g., Digital Video Broadcasting—Terrestrial) [3]. Urban and indoor wireless channels and underwater acoustic channels also suffer from impulsive noise [4]–[6]. In addition to telecommunication channels, sensors used in instrumentations introduce undesired signals such as artifacts and speckles to the measurements [7]. In images, "salt and pepper" noise is the most well-known version of the impulsive noise [8]. A standard median (SM) filter is usually preferred to reduce the salt-and-pepper noise in these 2-D signals [9]. In general, nonlinear methods have shown better performance in the reconstruction of signals with impulsive noise [10].

An SM filter manipulates all the samples of the signal, which can cause distortion in other "clean" samples. To address this problem, decision-based algorithms are adopted, in which the recovery of corrupted samples is performed after an impulsive noise detection step. One choice for detecting the impulses is to use hard decision. As an example, in [11], a hard-decision method based on ordered statistics is used to determine whether a sample is noisy. Another choice for detecting impulsive noise is to use soft-decision and fuzzy methods [12]–[16]. The method in [16], called noise adaptive soft-switching method, utilizes both the global and local statistics of image pixels. Depending on these statistics, the estimator switches between fuzzy weighted median and SM filters.

Due to impulsive noise, several samples of the signal are lost. The correction of the signal consists of both finding the positions of impulsive noises and estimating the original signal amplitude from the other clean samples. When the location of the impulses (corrupted samples) are known, the problem becomes the same as the erasure channel, which is extensively studied in [17] and [18] under the interpolation of missing samples. In [19], the more complicated problem of impulsive noise, where error locations are not known, is studied using DFT codes. In fact, the recovery of a band-limited signal corrupted by impulsive noise is equivalent to decoding error-correcting codes when the Galois field is extended to real and complex numbers. To clarify the concept, note that the zero coefficients in the discrete Fourier transform (DFT) of real/complex signals play the same role as the parity symbols in the Galois field codes; adding zero coefficients in the DFT domain (sampled frequency domain) is interpreted as oversampling in the time domain [20], [21]. Furthermore, it is also shown that the replacement of the DFT with the discrete cosine transform (DCT) would yield similar results [22]. One classical method of locating the position of errors is to compute the error locator polynomial (ELP) and then search for the roots. To show the strength of our method, we compare our results with the ones achieved by this method. In addition to impulsive noise, real/complex signals contain additive Gaussian noise; thus, the sensitivity of the reconstruction methods to this type of noise should also be considered [23]. It is known that iterative methods outperform other techniques when additive Gaussian noise is included [18].

In this paper, we focus on removing additive impulsive noise from a low-pass signal. High-pass frequencies (DFT coefficients) of the original signal are zero; thus, the respective frequencies of the available signal (original signal combined with noise) are only due to noise. Hence, we can restate our problem as follows. By having high-frequency content of an impulsive noise, we wish to remove it. We employ an iterative method where the initial detection of the impulsive noise locations is performed using an adaptive thresholding technique similar to the one used in a radar's constant false-alarm rate (CFAR) [24] detector. We refer to the finding of the impulsive locations as *detection*. The result of CFAR thresholding is used to make a soft decision on whether the sample is corrupted.

Manuscript received November 22, 2007; revised February 5, 2008. Current version published July 17, 2009. The review of this paper was coordinated by Associate Editor Dr. Jerome Blair.

S. Zahedpour, S. Feizi, and A. Amini are with the Advanced Communication Research Institute, Department of Electrical Engineering, Sharif University of Technology, Tehran 11365-9363, Iran (e-mail: zahedpour@ee.sharif.edu; feizi@ee.sharif.edu; arashsil@ee.sharif.edu).

M. Ferdosizadeh and F. Marvasti are with the Sharif University of Technology, Tehran 11365-9363, Iran (e-mail: mferdosi@ee.sharif.edu; marvasti@sharif.edu).

Digital Object Identifier 10.1109/TIM.2009.2016298

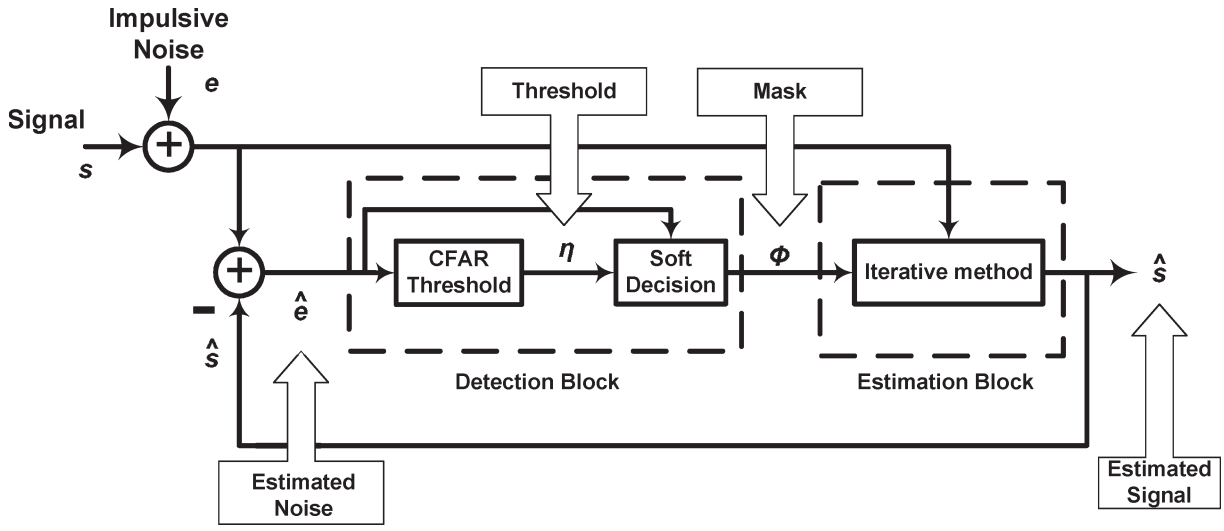

Fig. 1. RDE method.

Subsequently, this information is used in the interpolation of the signal amplitudes using an iterative method (referred to as signal *estimation*). The latter estimate is, in turn, used to improve the detection process, whereas the output of the improved detection is again fed to the estimation block. As this detection and estimation loop continues, we get better approximates of the signal.

The rest of this paper is organized as follows. In Section II, the proposed method is introduced. The detection and estimation blocks are discussed in Sections III and IV, respectively, whereas in Section V, the system is mathematically analyzed. In Sections VI and VII, alternative methods are presented and compared. Computer simulation results are discussed in Section VIII. Finally, Section IX concludes this paper.

II. Proposed Method

In this paper, we focus on removing additive impulsive noise $e[i]$ using the zeros in the DFT domain. To be specific, we define impulsive noise as an n-point discrete signal where, except for m samples ($m < n$), the rest are zero. Any probability distribution function (pdf) can be assumed for the values of the m nonzero samples; however, we assume Gaussian distribution for ease of analysis. Furthermore, the locations of these m nonzero samples are taken to be uniformly distributed among all the n samples. In some applications, instead of uniform Gaussian distribution, other models, e.g., the Bernoulli–Weibull [25] and Middleton's Class-A noise models [26], are employed.

We assume that the original signal $s[i]$ is real, which implies that its DFT is conjugate symmetric. For the reconstruction of each impulsive noise, we need two pieces of information (i.e., location and amplitude); thus, we require at least two independent equations that could be obtained by one zero in the DFT domain, with each zero describing two linear equations between time-domain samples: 1) one equation regarding the real part and 2) another equation for the imaginary part. However, due to the mentioned symmetry, each zero DFT coefficient in the positive frequencies is coupled with a zero in the negative frequencies that do not yield new equations. Thus, the "error correction capacity" of a given block (the maximum number of corrupted samples that we should reconstruct) can be defined as half the number of its zeros in the DFT domain; i.e., if the signal contains n_z zeros in the DFT domain, the error correction capacity is $n_z/2$. In this paper, error correction capacity and reconstruction capacity are interchangeably used. The terms *full capacity* and *half capacity* indicate the scenarios where the number of samples corrupted by impulsive noise is equal to or is half the reconstruction capacity, respectively.

Fig. 1 depicts the block diagram of our proposed method. As this figure suggests, the detection of impulse locations and estimation of signal amplitudes are successively used in a loop; this method is called recursive detection–estimation (RDE). To distinguish between the two different iterative methods used in this paper, we use the term "RDE step" for each time the detection–estimation loop proceeds (which should not be confused with iterations of the iterative method shown in Fig. 1). In each RDE step, the noise estimate $\hat{e}$ is improved using the approximated signal $\hat{s}$ that resulted from the previous RDE step by subtracting the estimated signal $\hat{s}$ from the noisy one. We have

$$\hat{e}_{\text{new}}[i] = r[i] - \hat{s}[i]. \tag{1}$$

The detection block functions as follows. If the amplitudes of impulsive noise are large enough, corrupted samples could be distinguished from the neighboring samples; thus, each detection is based on the difference between the sample and the average of its neighbors. This method is similar to the CFAR algorithm used in radar detectors. Hence, the detection block yields an adaptive threshold η using the impulsive noise estimate. As an example, the following equation describes the threshold obtained by the simple CFAR algorithm (not used in our method):

$$\eta_{\text{simple}}[i] = \frac{1}{2n_c}\left(\sum_{j=1}^{n_c}|\hat{e}_{\text{new}}[i-j]| + \sum_{j=1}^{n_c}|\hat{e}_{\text{new}}[i+j]|\right). \tag{2}$$

Based on the resulting threshold η, we can decide upon the noisiness of a sample either by hard decision or by soft decision. In the hard-decision scheme, a sample is regarded noisy when its amplitude is greater than the threshold, and vice versa. Alternatively, in our soft-decision scheme, instead of two possible labels "noisy" and "clean," we attenuate each sample with respect to its distance from the threshold ($|\hat{e} - \eta|$), which is, in fact, a measure of our certainty about its noisiness. As the difference between a sample and the adaptive threshold increases, the attenuating factor decreases to zero, which implies that the sample will likely be noisy; we denote the vector of the attenuating factors by *mask* ϕ, and the attenuation factor of each sample is called the respective mask coefficient $\phi[i]$. We have

$$\text{masked noisy signal} = \phi[i] \times r[i], \qquad 1 \leq i \leq n. \quad (3)$$

In each RDE step, as the accuracy of the impulsive noise estimate improves, we obtain a new mask. Computer simulations confirm that, in the initial RDE steps, the soft-decision method leads to better outputs than the hard-decision method. As the number of RDE steps increases, better estimates of the impulsive noise are obtained. This case makes it possible to shift the soft-decision threshold to the hard one (using a parameter of ϕ called α), which, in turn, makes the mask more accurate.

After detecting the impulsive noise locations, the amplitude of the corrupted sample is estimated. The estimation is based on interpolation of the amplitude using the surrounding clean samples. Multiplying the noisy signal by the mask and filtering the result is a simple method of approximating the original signal. Although this simple method will likely alleviate the noise effect, it certainly distorts other clean samples. To compensate for the distortion, we use an iterative method (shown as "iterative method" in Fig. 1) inside the estimator in each RDE step. To clarify the roles of RDE loop and the iterative method, it should be emphasized that the RDE steps improve the detection of corrupted samples (locations), whereas the iterative method enhances the estimation of original signal amplitudes. The algorithm of the proposed method can be summarized as follows.

1) Approximate the impulsive noise $\hat{e}$ by subtracting the estimated signal from the noisy one (1). In the first RDE step, no estimate about the signal is available; thus, signal is assumed to be zero.
2) Generate thresholds η using censored mean level (CML)–CFAR in Section III-A.
3) Generate a mask ϕ using the soft-decision detector (with parameter α) in Section III-B.
4) Use the mask in conjunction with the iterative method in Section IV to improve the estimate of the signal.
5) Return to the first step. In the soft-decision function of Step 3, increase parameter α to shift the soft-decision function to the hard one. Increase the number of iterations in Step 4 to further improve the signal estimation.

In the next two sections, details of the detection and estimation blocks are discussed.

III. Impulsive Noise Detection

As previously described, we introduce a multiplicative mask to suppress the impulses while trying to keep the clean samples unchanged. We only have an estimate of the impulse locations; thus, two types of errors are likely to happen. A *missed detection* occurs if a corrupted sample is not detected, whereas a *false alarm* occurs if a legitimate sample is detected as noise. Two important techniques are incorporated to alleviate these effects: 1) the use of CFAR and 2) the employment of soft decision. We explain these techniques in the following sections.

A. Adaptive Impulsive Noise Detection Using CFAR

The threshold for detecting impulsive noise can either be adaptive or non adaptive. In the nonadaptive method, a fixed threshold is used to compare the amplitude of the sample under scrutiny to determine whether an impulse at that instant exists. This threshold is obtained using the statistical properties of the signal and noise. On the other hand, the more sophisticated thresholding schemes incorporate the amplitude of the adjacent samples to obtain adaptive thresholds. The CFAR algorithm is an example of an adaptive thresholding method used in radar detectors based on the Neyman–Pearson criterion [27]. In radar applications, the detector detects the target in the presence of noise and clutter, which is equivalent to the detection of impulsive noise locations among other clean samples. Thus, the techniques used in radar detectors can be adopted for the problem at hand. Fig. 2 depicts a simple CFAR detector. The CFAR processing block may be either amplitude averaging (cell Averaging–CFAR) as suggested in (2) or a more complicated combination of adjacent samples. In this paper, we use a CML–CFAR. In the kth-order CML–CFAR of length $2n_c$, among the $2n_c$ adjacent cells, k of the smallest amplitudes are averaged, and the other $2(n_c - k)$ samples (which may contain impulses) are ignored. In other words, if $|\hat{e}[j_1]| \leq \cdots \leq |\hat{e}[j_{2n_c}]|$, where $\{j_1, \ldots, j_{2n_c}\} = \{i - n_c, \ldots, i + n_c\}/\{i\}$, we have

$$\eta[i] = \frac{1}{k} \sum_{l=1}^{k} |\hat{e}[j_l]| \,. \quad (4)$$

The reason that we use CML–CFAR is to reduce the probability that impulses contribute in the averaging when some of them are present in adjacent cells.

B. Soft Decision Versus Hard Decision

The detection stage is not an error-free process in the early RDE steps, particularly when the amplitudes of the impulses are small compared to the signal amplitudes. When the hard-decision method is employed, the mask is either zero or one at each sample; thus, some samples are erased. The optimistic point of view is that only the noisy samples are lost; however, if we have mistakenly discarded a number of clean samples (resulting in false alarms), this error may or may not be recoverable, depending on the number of impulses with respect to the number of zeros in the DFT domain. On the other hand, when

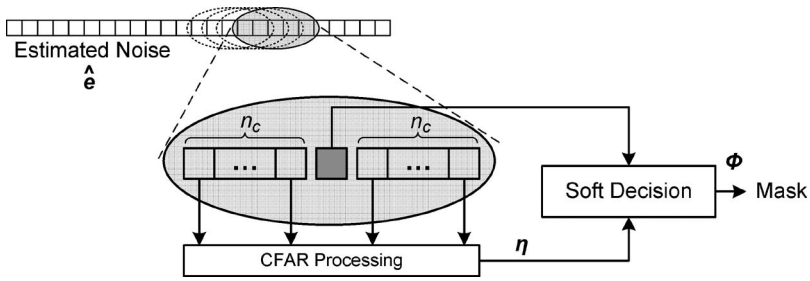

Fig. 2. Typical CFAR detector and decision block.

we use soft decision, even when the detector makes a number of false alarms, the attenuation can be compensated for without any need of extra zeros in the DFT domain. The disadvantage of the "soft-decision" method is the low convergence rate in the signal estimation block, even when good estimates of the impulsive noise locations are available. To overcome this drawback, we gradually change the soft-decision method to the hard threshold as the number of RDE steps (estimation fidelity of the noise locations) increases. To summarize, using hard decision within the detection block, a binary mask is generated, i.e., the value of the mask at each sample is zero if the sample is detected as noisy; otherwise, the value is one. On the other hand, the soft-decision block generates a real number between zero and one, depending on the certainty of the detector.

Simulation results suggest that the mask function of the form

$$\phi\left(\hat{e}[i], \eta[i]\right) = e^{-\alpha|\hat{e}[i]-\eta[i]|} \tag{5}$$

performs well, where $\hat{e}$ is the estimated error, η is the threshold generated by CFAR [28], and α is the softness order of the detection block. The suggested $\phi(\hat{e}, \eta)$ approaches one as $\hat{e} - \eta$ tends to zero. The parameter α is gradually increased through RDE steps to change the soft-decision method into the hard-decision method, which, in turn, increases the convergence rate of the estimator.

IV. Signal Estimation

In the rest of this paper, we assume that the original signal $s[i]$ is discrete and low pass with n_z zeros in the DFT domain. Thus, ideally, we should detect and reconstruct $n_z/2$ corrupted samples. Mathematically, we should solve an underdetermined system of equations [29] with some additional constraints (the number of impulses does not exceed $n_z/2$, and each impulse corrupts only one sample). Let $r[i] = s[i] + e[i]$, where $r[i]$ is the noisy signal, $s[i]$ is the original signal, and $e[i]$ is the impulsive noise. We have

$$\begin{bmatrix} R_1 \\ R_2 \end{bmatrix} = \begin{bmatrix} S_1 \\ 0 \end{bmatrix} + \begin{bmatrix} E_1 \\ E_2 \end{bmatrix} = \begin{bmatrix} S_1 + E_1 \\ E_2 \end{bmatrix} \tag{6}$$

where the capital letters denote the respective signals in the DFT domain. R_1, S_1, and E_1 are the low-pass components of the R, S, and E signals, respectively, whereas R_2 and E_2 are the high-pass parts (the high-pass component of S is zero). E and e are related to each other by the DFT matrix $\mathbf{\Delta}$ as

$$E = \mathbf{\Delta}_{n\times n} \cdot e \tag{7}$$

where

$$\mathbf{\Delta} = \begin{pmatrix} 1 & 1 & 1 & \dots & 1 \\ 1 & e^{-j\frac{2\pi}{n}} & e^{-j\frac{2\pi}{n}2} & \dots & e^{-j\frac{2\pi}{n}(n-1)} \\ \vdots & \vdots & \vdots & \ddots & \vdots \\ 1 & e^{-j\frac{2\pi}{n}(n-1)} & e^{-j\frac{2\pi}{n}2(n-1)} & \dots & e^{-j\frac{2\pi}{n}(n-1)^2} \end{pmatrix}. \tag{8}$$

To reconstruct the signal, we should solve the underdetermined system of equations. We have

$$E_2 = \mathbf{\Delta}_{n_z\times n} \cdot e \tag{9}$$

where $\mathbf{\Delta}_{n_z\times n}$ contains the n_z rows of $\mathbf{\Delta}$, which are zero in S. In Section IV-A, we introduce a general iterative method to synthesize the inverse of a system. As mentioned in Section II, these iterations are performed in the estimation block to approximate the original signal (in each RDE step) and should not be confused with the RDE (external) loop.

A. Successive Signal Approximations Using an Iterative Method

The iterative method in [18] is a general approach for approximating the inverse of a class of invertible operators in a finite number of iterations. Furthermore, for a wider class of invertible and linear noninvertible operators, the convergence of this method to the pseudo-inverse solution has been shown [30]. The invertible operator can be nonlinear and/or time varying.

We denote the operator whose inverse we intend to find by G. In addition, $y = G \cdot x$ means that y is the output of the operator when x is the input. The purpose of the iterative method is to estimate x when y and G are known, i.e., approximating G^{-1}. Using the operator algebra and denoting the identity operator by I, we have

$$G^{-1} = \frac{\lambda}{I - (I - \lambda G)} = \lambda \sum_{i=0}^{\infty} (I - \lambda G)^i. \tag{10}$$

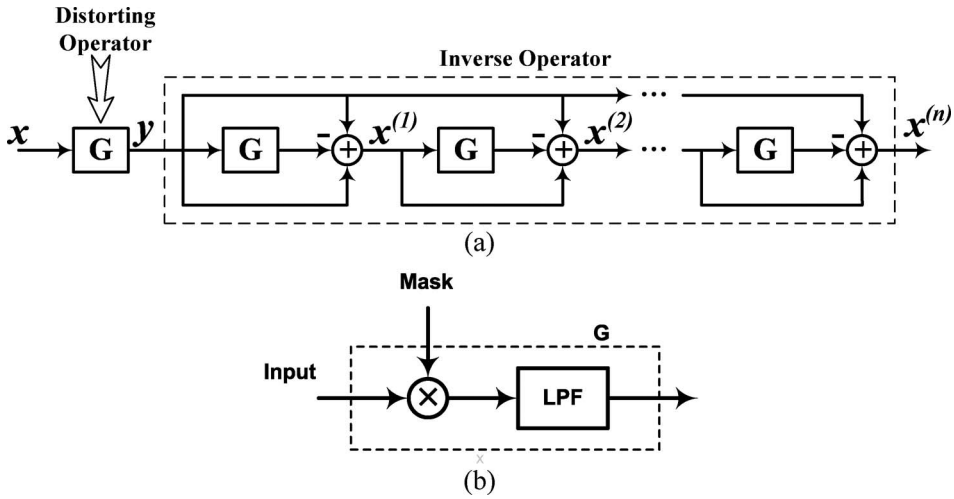

Fig. 3. (a) Block diagram of the iterative method with $\lambda = 1$. (b) Model of the distortion block G in our specific application.

The assumption of $\|I - \lambda G\| < 1$ is necessary for convergence, where $\|\cdot\|$ is the ℓ_2 norm. Thus

$$x = \lambda \sum_{i=0}^{\infty} (I - \lambda G)^i \cdot y. \tag{11}$$

The output of each iteration step is equivalent to truncating the aforementioned series. The output of the $(k+1)$th iteration is

$$\begin{aligned} x^{(k+1)} &= \lambda \sum_{i=0}^{k+1} (I - \lambda G)^i \cdot y \\ &= \lambda y + (I - \lambda G) \cdot \lambda \sum_{i=0}^{k} (I - \lambda G)^i \cdot y. \end{aligned} \tag{12}$$

$y = G \cdot x$; thus, (12) can recursively be written as

$$x^{(k+1)} = x^{(k)} + \lambda G \cdot \left(x - x^{(k)} \right). \tag{13}$$

In the following, we refer to (13) as the *iterative method*. It is obvious that the condition $\|I - \lambda G\| < 1$ is met only for a specific range of λ (this range is normally $0 \leq \lambda < 2$). Moreover, decreasing $\|I - \lambda G\|$ by increasing λ will result in a faster convergence rate. Hence, λ determines whether the method converges and, if it does, how fast it converges. The block diagram of (13) is shown in Fig. 3(a). For the special case in this paper, we briefly present the proof of the convergence for a linear contraction operator $G(\|G\| < 1)$. To show this convergence, assume that

$$z^{(k)} = x - x^{(k)}. \tag{14}$$

Thus

$$z^{(k+1)} = x - x^{(k+1)} = z^{(k)} - \lambda \left(G \cdot \left(x - x^{(k)} \right) \right) \tag{15}$$

or

$$z^{(k+1)} = D \cdot z^{(k)} \tag{16}$$

where $D = I - \lambda G$. For $0 < \lambda < 2$, using the contraction property of G, we have $\|D\| < 1$, and therefore, $z^{(k+1)} \to 0$, which results in $x^{(k)} \to x$.

In the following discussion, we apply the aforementioned iterative method to estimate the amplitude of the corrupted samples using the mask generated by the detection block as part of the G operator. The detection block in Section III generates a mask vector that contains information about the locations of the impulsive noise. By employing the mask, the iterative method described by (13) can be used to recover the corrupted samples. The distortion operator applied for these iterations is depicted in Fig. 3(b). In addition to the mask, a low-pass filter is employed, which helps in the reconstruction of the corrupted samples. Both the mask and the low-pass filter are linear contraction operators; consequently, the depicted distortion block is also a linear contraction that validates the convergence to the solution (see Section IV-A). In the early RDE steps, the outputs of the detection block are not reliable; thus, a small number of iterations are used. In contrast, when better approximations of the signal are obtained (at higher RDE steps), the increase in the number of iterations yields better performance.

In the next section, a mathematical analysis of the proposed method is discussed.

V. Analysis of the Proposed Method

In this section, the effect of the iterative method on both the signal and the impulsive noise is investigated. In our application, G is linear; thus, its operation can be modeled, in general, by the multiplication of a matrix $\mathbf{G}$, i.e.,

$$\mathbf{G} = \mathbf{\Delta}^{-1} \cdot \mathrm{diag}(\underbrace{1, \ldots, 1}_{n-n_z}, \underbrace{0, \ldots, 0}_{n_z}) \cdot \mathbf{\Delta} \cdot \mathbf{M} \tag{17}$$

where $\mathbf{M}$ is a diagonal matrix with the values of the mask on its main diagonal, and $\mathbf{\Delta}$ is the DFT coefficients matrix in (8). In addition, by $\mathrm{diag}(\cdot)$, we mean a diagonal matrix with diagonal elements, as given inside the parenthesis.

This matrix multiplication for the signal and impulsive noise can separately be considered. First, the behavior of the signal

through the iterations is examined. By using (14), (13) can be written as

$$\mathbf{z}^{(k+1)} = (\mathbf{I} - \lambda\mathbf{G})\mathbf{z}^{(k)}. \tag{18}$$

The spectrum of the signal, after multiplying by the mask, spreads over the frequency; hence, by the use of a low-pass filter, we moderately improve the distorted signal, because the original signal is assumed to be low pass. However, Amini in [30] and [31] has shown that, for matrices in the same form as $\mathbf{G}$, the iterative method converges, even without the low-pass filtering. Consequently, the role of the filter can be viewed as an accelerating tool. Thus, to obtain a crude approximation of the convergence rate, we ignore the low-pass filter. Hence, (18) can be rewritten as

$$\mathbf{z}^{(k+1)} = (\mathbf{I} - \lambda\mathbf{M})\mathbf{z}^{(k)} \tag{19}$$

$$= (\mathbf{I} - \lambda\mathbf{M})^{k+1}\mathbf{z}^{(0)}. \tag{20}$$

All the elements of $\mathbf{I} - \lambda\mathbf{M}$ are between zero and one; thus, $\mathbf{z}^{(k)} \to 0$ as $k \to \infty$.

Let m_i be the ith element of the main diagonal of $\mathbf{M}$. After l iterations, the ith element of the $(\mathbf{I} - \lambda\mathbf{M})^l$ is $(1 - \lambda m_i)^l = e^{l.\ln(1-\lambda m_i)}$; thus, the ith element on the diagonal exponentially decays as l increases with the time constant $(1/\tau_i) = \ln(1/1 - \lambda m_i)$. To have a single time constant, we use the following average:

$$\frac{1}{\tau_{\text{av}}} = E\left\{\sum_i \frac{1}{\tau_i}\right\} \tag{21}$$

where τ_{av} is the average time constant, and $E\{\cdot\}$ denotes the expected value operator.

To continue our analysis, we focus on the mask values. Using the exponential soft-decision method, we have

$$m_i = e^{-\alpha|r[i]-\hat{s}[i]|} = \begin{cases} e^{-\alpha|s[i]+e[i]-\hat{s}[i]|}, & \text{r[i] is noisy} \\ e^{-\alpha|s[i]-\hat{s}[i]|}, & \text{otherwise} \end{cases} \tag{22}$$

where $\hat{s}$ is the estimate of s, and e represents the impulsive noise amplitude. To calculate τ_{av}, the pdf of $s - \hat{s}$ and $s - \hat{s} + e$ should be calculated. We assume that the input signal has zero-mean Gaussian distribution. The estimation that we use are linear; thus, $s[i] - \hat{s}[i]$ also has zero-mean Gaussian distribution with the variance of σ^2_{est}. With a similar assumption about the noise distribution (zero-mean Gaussian with variance σ_e^2) and the independence of the noise and the signal, $s - \hat{s} + e$ also has zero-mean Gaussian distribution with variance σ_n^2. By the numerical calculation of τ_{av} in the simulations, we have found out that the best linear fit with respect to the minimum-mean-square-error criterion is

$$\tau_{\text{av}} = 5.43 + 15\alpha\left(p\sigma_n + (1-p)\sigma_{\text{est}}\right) \tag{23}$$

where p is the probability that a sample contains an impulsive noise. Now, we can write the following approximation:

$$\mathbf{z}^{(l)} = \underbrace{(\mathbf{I} - \lambda\mathbf{M})^l}_{\approx e^{-l/\tau_{\text{av}}}\cdot\mathbf{I}}.\mathbf{z}^{(0)} \Rightarrow \left\|\mathbf{z}^{(l)}\right\| \approx e^{-\frac{l}{\tau_{\text{av}}}}\left\|\mathbf{z}^{(0)}\right\|. \tag{24}$$

In other words, excluding the impulsive noise, the improvement in the signal in each iteration can be approximated by $20\tau_{\text{av}}^{-1}\log(e)$ dB.

Now, we consider the effect of the iterations on the noisy part. We decompose the noise into low- and high-pass parts as follows:

$$\mathbf{e}_{\text{LP}} = \left(\mathbf{\Delta}^{-1}\cdot\text{diag}(\underbrace{1,\ldots,1}_{n-n_z},\underbrace{0,\ldots,0}_{n_z})\cdot\mathbf{\Delta}\right)\cdot\mathbf{e}$$

$$\mathbf{e}_{\text{HP}} = \left(\mathbf{\Delta}^{-1}\cdot\text{diag}(\underbrace{0,\ldots,0}_{n-n_z},\underbrace{1,\ldots,1}_{n_z})\cdot\mathbf{\Delta}\right)\cdot\mathbf{e}. \tag{25}$$

It is clear that $\mathbf{e} = \mathbf{e}_{\text{LP}} + \mathbf{e}_{\text{HP}}$. The nonzero frequency components of $\mathbf{e}_{\text{LP}}$ coincide with the original low-pass signal; thus, the iterative method cannot distinguish these two signals. In other words, if the soft-decision method with a large number of iterations is used, $\mathbf{e}_{\text{LP}}$ will be a dominant additive part. On the other hand, due to the use of the low-pass filter, $\mathbf{e}_{\text{HP}}$ vanishes. Hence, at the end of ∞ iterations, we will have an additive noise part with variance

$$\begin{aligned} &E\left\{\|\mathbf{e}_{\text{LP}}\|^2\right\} \\ &\quad= E\left\{\mathbf{e}_{\text{LP}}^H\cdot\mathbf{e}_{\text{LP}}\right\} \\ &\quad= E\left\{\mathbf{e}^H\cdot\mathbf{\Delta}^{-1}\cdot\text{diag}(\underbrace{1,\ldots,1}_{n-n_z},\underbrace{0,\ldots,0}_{n_z})\cdot\mathbf{\Delta}\cdot\mathbf{e}\right\} \\ &\quad= \text{Tr}\left\{E\{\mathbf{e}\cdot\mathbf{e}^H\}\cdot\mathbf{\Delta}^{-1}\cdot\text{diag}(1,\ldots,1,0,\ldots,0)\cdot\mathbf{\Delta}\right\} \\ &\quad= p\cdot\sigma_e^2\cdot\text{Tr}\left\{\mathbf{\Delta}^{-1}\cdot\text{diag}(1,\ldots,1,0,\ldots,0)\cdot\mathbf{\Delta}\right\} \\ &\quad= (n-n_z)p\sigma_e^2. \end{aligned} \tag{26}$$

Thus, the impulsive noise power after ∞ iterations is expected to decrease by $-10\log(1-(n_z/n))$ dB (because the average noise power before the iteration is $np\sigma_e^2$). It should be emphasized that, if hard decision is used (at higher RDE steps), the aforementioned equations are not valid, and noise analysis should be performed by checking the error probability of the location detector. Another important issue is that the aforementioned equations are comparing the noise before and at the end of ∞ iterations. In fact, the power of the noise after the first iteration is lower than the power of the noise after the last iteration; however, the quality of the signal is remarkably improved after the last iteration. Therefore, we expect to get a net gain in the signal to impulsive noise ratio after a finite number of iterations. Empirically, each iteration improves the signal component more than the degradation due to the impulsive noise reconstruction.

We finish this section by investigating the effect of the mask on the noisy part. The noise is impulsive; thus, only the value of the mask at the locations of the impulses is important. For an impulse at the ith sample, the value of the mask is equal

to $e^{-\alpha|s[i]+e[i]-\hat{s}[i]|}$. Thus, the amplitude of this impulse after multiplication by the mask is

$$\tilde{e}[i] = e[i].e^{-\alpha|s[i]+e[i]-\hat{s}[i]|}. \tag{27}$$

We have previously assumed that both noise and $s[i]-\hat{s}[i]$ are Gaussian distributed random variables with zero mean and variance σ_e^2 and σ_{est}^2, respectively. Thus

$$\begin{aligned}
E\left\{\tilde{e}^2[i]\right\} &= \int_{-\infty}^{\infty}\int_{-\infty}^{\infty} n^2 \cdot e^{-2|x+n|}\frac{e^{-\frac{x^2}{2\sigma_{\text{est}}^2}}\cdot e^{-\frac{n^2}{2\sigma_e^2}}}{2\pi\sigma_e\sigma_{\text{est}}}\,dx\cdot dn \\
&< \int_{-\infty}^{\infty}\int_{-\infty}^{\infty} n^2 \cdot e^{2|x|-2|n|}\frac{e^{-\frac{x^2}{2\sigma_{\text{est}}^2}}\cdot e^{-\frac{n^2}{2\sigma_e^2}}}{2\pi\sigma_e\sigma_{\text{est}}}\,dx\cdot dn \\
&= \int_{-\infty}^{\infty} n^2\cdot e^{-2|n|}\frac{e^{-\frac{n^2}{2\sigma_e^2}}}{\sqrt{2\pi}\sigma_e}\cdot dn \int_{-\infty}^{\infty} e^{2|x|}\frac{e^{-\frac{x^2}{2\sigma_{\text{est}}^2}}}{\sqrt{2\pi}\sigma_{\text{est}}}\cdot dx \\
&= \sigma_e^2 e^{2\sigma_e^2}Q(2\sigma_e)8\sigma_e^2 + 2 - \frac{4\sigma_e}{\sqrt{2\pi}}2e^{2\sigma_{\text{est}}^2}Q\left(-2\sigma_{\text{est}}^2\right) \\
&\approx \sigma_e^2 e^{2\sigma_e^2}Q(2\sigma_e)8\sigma_e^2 + 2 - \frac{4\sigma_e}{\sqrt{2\pi}}e^{2\sigma_{\text{est}}^2} \\
&< 0.41\sigma_e^2\cdot e^{2\sigma_{\text{est}}^2}
\end{aligned} \tag{28}$$

where

$$Q(x) = \int_x^{\infty}\frac{e^{-\frac{y^2}{2}}}{\sqrt{2\pi}}\cdot dy. \tag{29}$$

Hence, when a good estimator is present ($\sigma_{\text{est}} < 2/3$), the variance of the masked noise falls below the variance of the noise before the mask. We have

$$E\left\{\tilde{e}^2[i]\right\} < \sigma_e^2. \tag{30}$$

Furthermore, by low-pass filtering the masked output, this power is again decreased by discarding the high-frequency components. To summarize, we have shown that the SNR of the reconstructed signal is at least

$$\text{SNR}_{\min} = \frac{N\sigma_s^2}{(n-n_z)p\sigma_e^2} \tag{31}$$

where σ_s is the standard deviation of the signal.

VI. Alternative Method for Detecting Impulsive Noise Locations

In [32], a decoding technique for DFT-based error control codes using ELP is devised. In this section, we combine the ELP decoding with the proposed iterative method. Let us assume that the original signal $s[i]$ is an n-point discrete signal with n_z contiguous zeros in the DFT domain. Thus, from the coding point of view, we are using an $(n, n-n_z)$-code with the ability to correct up to $t=(n_z/2)$ random errors. We denote the impulsive noise and the corrupted signals by $e[i]$ and $r[i]$, respectively. The impulsive noise $e[i]$ is assumed to be nonzero, at most, at $(n_z/2)$ samples. The corrupted signal and the impulsive noise are related to each other by

$$r[i] = s[i] + e[i] \tag{32}$$

$$R[k] = S[k] + E[k] \tag{33}$$

where the capital letters denote the DFT domain. Assume that

$$S[k] = 0 \quad \text{for} \quad k_0 \le k \le k_0 + 2t - 1. \tag{34}$$

When $n_e \le t$ errors are present in the received block, the ELP is defined as

$$H(\Omega) = \prod_{k=1}^{n_e}\left(\Omega - \exp\left(j\frac{2\pi}{n}i_k\right)\right) \tag{35}$$

$$= \sum_{k=0}^{t} h_k\cdot\Omega^k \tag{36}$$

where $\{i_k\}_{k=1}^{n_e}$ are the location of errors, and $h_k = 0$ for $n_e < k \le t$ and $h_{n_e} = 1$. In fact, the roots of this polynomial are exponentially related to the location of errors, i.e., $H(\Omega_k) = 0$ for $\Omega_k = \exp(j(2\pi/n)i_k)$. We have

$$H(\Omega_k) = h_t\Omega_k^t + h_{t-1}\Omega_k^{t-1} + \cdots + h_0 = 0. \tag{37}$$

Using the aforementioned equalities for $1 \le k \le n_e$, we can write

$$\begin{aligned}
0 &= \sum_{k=1}^{n_e} H(\Omega_k)\cdot e(i_k)\cdot\exp\left(-j\frac{2\pi\cdot r}{n}i_k\right) \\
&= h_t E[r-t] + h_{t-1}E[r+1-t] + \cdots + h_0 E[r].
\end{aligned} \tag{38}$$

The good point is that $E[k]=R[k]$ for $k_0 \le k \le k_0+2t-1$, and therefore, the value of $E[k]$s are known in this range. If we set $k_0 + t \le r \le k_0 + 2t - 1$ in (38), we obtain a system of t equations with $t+1$ unknowns (h_k coefficients). These equations yield a unique solution for the polynomial, with the additional condition that the last nonzero h_k is equal to one. Instead of matrix inversion, a more efficient method for solving these equations is the Berlekamp–Massey algorithm. Finding the coefficients, we have to search for the roots. The roots of $H(\Omega)$ are of the form $\exp(j(2\pi/n)i_k)$; thus, the inverse DFT (IDFT) of the $\{h_k\}_{k=0}^{t}$ can be used. Before performing IDFT, we have to pad $n-1-t$ zeros at the end of the $\{h_k\}_{k=0}^{t}$ sequence to obtain an n-point signal. We refer to the new signal (after IDFT) as $\{H_k\}_{k=0}^{n-1}$. Each zero in $\{H_k\}$ represents an error in $r[k]$ at the same location.

We use the aforementioned method in real numbers; thus, exact zeros of $\{H_k\}$s are rarely observed. Consequently, we threshold the $|H_k|$s to find the zeros. Alternatively, $|H_k|$s can be used as a mask for soft decision; in this case, thresholding is not needed.

VII. Hard Decision and Filtering

The simplest method for eliminating the impulsive noise is to hard limit the noisy signal and then apply a low-pass filter to the output of the hard limiter. This method does not efficiently use the redundancy in the signal; nevertheless, it can be viewed as a crude reconstruction algorithm. To have the best performance, we optimize the threshold for the hard limiter. Let us assume that the amplitudes of the signal and the impulsive noise have the PDF's $N(0,\sigma_s^2)$ and $N(0,\sigma_e^2)$, respectively. Moreover, p denotes the probability that a sample is noisy, and η represents the threshold for hard limiting. The probability of error is

$$P_e = (1-p)e^{\frac{-\eta^2}{2\sigma_s^2}} + p\left(1 - e^{\frac{-\eta^2}{2(\sigma_s^2+\sigma_e^2)}}\right). \tag{39}$$

Then, the optimum threshold (to minimize P_e) can be derived by differentiating P_e with respect to the threshold level, i.e.,

$$\frac{\partial}{\partial \eta} P_e = 0. \tag{40}$$

Hence

$$\eta_{\text{opt}} = \sigma_s \sqrt{2(1+\text{SNR}) \cdot \ln\left(\frac{1-p}{p} \cdot \frac{1+\text{SNR}}{\text{SNR}}\right)} \tag{41}$$

where $\text{SNR} = \sigma_e^2/\sigma_s^2$. To have an optimum threshold, p should satisfy the following equation:

$$p \le \frac{1+\text{SNR}}{1+2\text{SNR}}. \tag{42}$$

VIII. Simulation Results

To prove the effectiveness of the proposed method, various simulations were conducted. In all simulations, the signal is a filtered white Gaussian pseudorandom signal. We have also tested signals with uniform distribution, which yielded similar results.

Fig. 4 shows the simulation results when the process of hard limiting and low-pass filtering is repeated. For the number of impulses, we considered both full capacity (half the number of DFT zeros of the signal) and half capacity (one fourth the number of DFT zeros of the signal). It is observed that, in the case of full capacity, the improvement after 10 RDE steps is below 10 dB.

As previously predicted, the soft-thresholding method in Section III, with repetition of detection and estimation processes, as shown in Fig. 5, yields much better results for full capacity (the maximum number of impulses that can be corrected). To find the mask function, both the simple soft-decision method and CFAR are used. Fig. 5 suggests that, by adding CFAR to the soft-decision method, the recovery is enhanced. When we use CFAR, we require a fewer number of iterations in the amplitude estimation steps of the impulsive noise; thus, CFAR adds little computational overhead on the overall complexity of the algorithm.

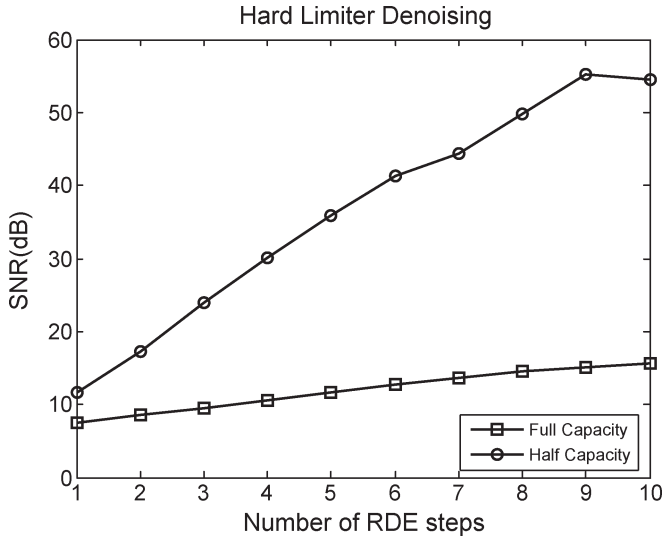

Fig. 4. Multiple RDE steps using hard decision and simple detector.

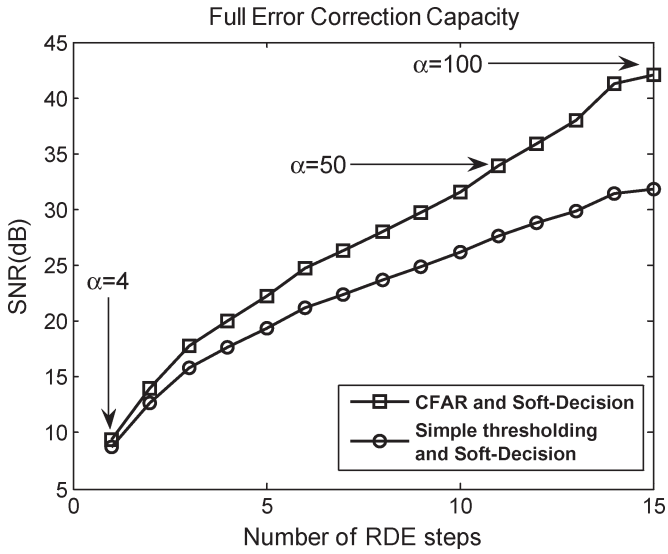

Fig. 5. Comparison of CFAR and simple soft decision at full capacity.

The α parameter in the soft-decision method and the number of iterations in the estimator of the proposed method are varied from one RDE step to another, as shown in Table I. These numbers are empirically derived and are not claimed to be optimal. As it has been observed, the α parameter is nondecreasing; thus, the decision rule is gradually changed from soft to hard decision as RDE steps proceed. Incidentally, the number of iterations in the estimator increases as the signal estimate becomes more reliable at higher steps. The CFAR parameters n_c and k were chosen to be 20 and 15, respectively. In the iterative method, parameter λ is set to one.

If the number of impulses exceeds the reconstruction capacity, the SNR of the reconstructed signal is gracefully degraded, because the iterative method leads to the pseudoinverse solution [30], [31]. Fig. 6 depicts the SNR of the reconstructed signal when the number of the errors introduced by the impulsive channel is 15% more than the theoretical reconstruction

TABLE I
SOFT-DECISION PARAMETER AND THE NUMBER OF ITERATIONS

RDE step	1	2	3	4	5	6	7	8	9	10	11	12	13	14	15
α	4	6	10	10	14	20	20	25	30	40	50	60	70	70	100
No. of Iterations	50	50	50	50	100	100	100	100	100	100	200	200	200	200	200

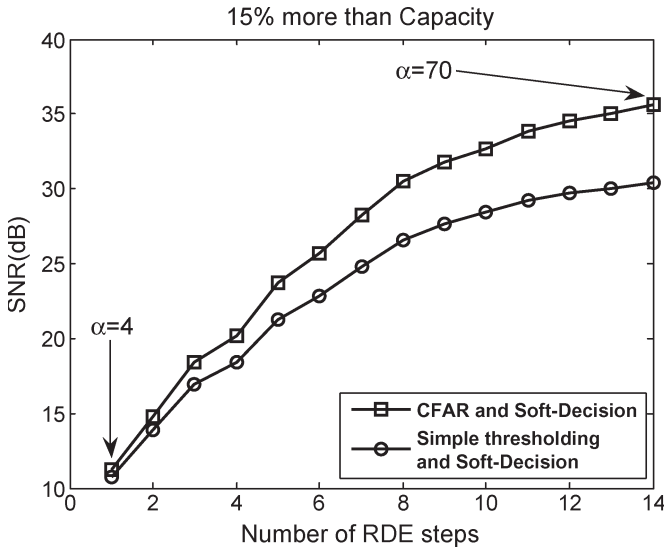

Fig. 6. SNR of the denoised signal when the error rate exceeds the reconstruction capacity by about 15%.

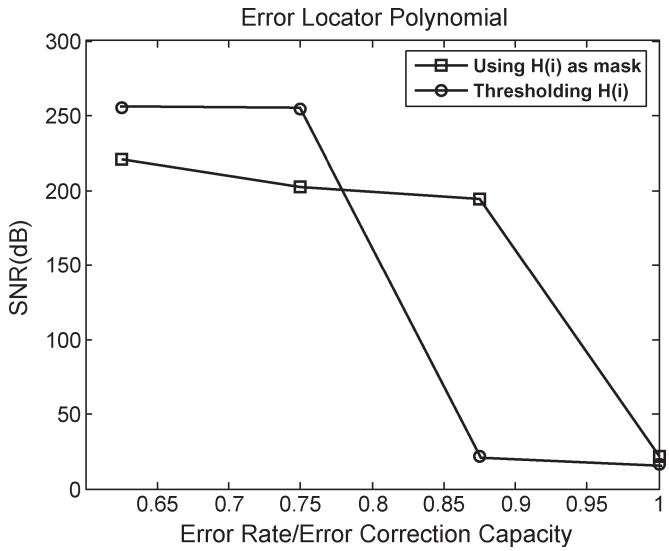

Fig. 7. SNR of the denoised signal using ELP to generate mask.

capacity. It is shown that the SNR gracefully degrades compared to Fig. 5, but the algorithm does not diverge.

We have also simulated the ELP method in Section VI to detect error locations and estimated the signal using 500 iterations. With the use of the Chebychev acceleration method [33], we can reduce this number to one third. For the hard-decision ELP method, we have generated the mask by thresholding $|H_k|$, which has yielded a binary mask. The threshold is set to a small number to determine the locations of zeros. For $|H_k|$s smaller than the threshold, an error is assumed at that location. For the soft-decision ELP method, we use $|H_k|$ as the mask. The performance of these methods is depicted in Fig. 7.

These methods do not perform as well as the previous method at full capacity; however, it performs better for low error rates.

In Table II, we compare the relative complexity (computer time) and achievable SNR's for various methods at different impulsive noise rates. We have used thresholding in conjunction with low-pass filtering as the most simple reconstruction method (with complexity 1), and the complexity of other methods are compared to this simple method. As another simple method, median filtering is also used for comparison. This table clearly shows that, at full capacity, the soft-decision method with the iterative technique gives the best performance in terms of the SNR. The performance of ELP is less than half in the SNR with 10 times more in complexity. However, at half the capacity, ELP performs very well.

We have initially assumed that each impulse corrupts only one sample of the signal. However, due to the characteristics of noise source, it is possible that consecutive impulses (burst error) occur. By increasing the number of consecutive impulses, the condition number of the matrix G (introduced in Section V) also increases, and consequently, the convergence rate decreases. For matrices with a poor condition number, additive white noise or finite numerical precision may lead to divergence. In our simulations, we can recover bursts of size 4.

If, prior to the transmission of the signal, characteristics of the noise source (channel) are known, interleaving in time or frequency (sorted DFT [34]) can improve the robustness of the method in case of bursty impulses. The ELP method in Section VI can also be used to find the errors using sorted DFT.

IX. CONCLUSION

In this paper, we have proposed a new method for impulsive noise cancellation. In this method, with the use of recursive detection/estimation steps, we approach the theoretical upper bound of reconstruction capacity. The SNR of the reconstructed signal can be improved by increasing the number of detection/estimation steps and increasing the number of iterations in each estimation block. Soft decision and adaptive thresholding (CFAR) are used in the detection procedure, which enhances the performance. Simulation results show that the SNR of the reconstructed signal gradually degrades if the number of impulses exceeds the theoretical reconstruction capacity. We have also used the ELP method in conjunction with the iterative method to estimate the corrupted samples of the signal. The SNR performance of the ELP method is higher than the RDE method for low error rates but is much worse at full capacity, with a complexity that is higher by an order of magnitude.

TABLE II
RELATIVE COMPLEXITY OF THE METHODS AND THE RESULTING SNR

Method	SNR(dB) at full capacity	SNR(dB) at 15% overloaded	SNR(dB) at 70% capacity	Complexity
Thresholding and LPF	7	6.8	10	1
Median Filter	18	13.5	20	1000
Non-Adaptive Hard-dec.	13	9.5	19	500
CFAR Soft-dec	42	35.1	50	5000
ELP	20	2	250	50000

The ideas used in this paper can also be used to other real field error-correcting codes (e.g., DCT, wavelet, and random codes), sparse component analysis, and OFDM clipping noise removal.

REFERENCES

[1] M. Zimmermann and K. Dostert, "Analysis and modeling of impulsive noise in broadband powerline communications," *IEEE Trans. Electromagn. Compat.*, vol. 44, no. 1, pp. 249–258, Feb. 2002.

[2] D. Levey and S. McLaughlin, "The statistical nature of impulse noise interarrival times in digital subscriber loop systems," *Signal Process.*, vol. 82, no. 3, pp. 329–351, Mar. 2002.

[3] M. Sanchez, L. de Haro, M. Ramon, A. Mansilla, C. Ortega, and D. Oliver, "Impulsive noise measurements and characterization in a UHF digital TV channel," *IEEE Trans. Electromagn. Compat.*, vol. 41, no. 2, pp. 124–136, May 1999.

[4] D. Middleton, "Non-Gaussian noise models in signal processing for telecommunications: New methods an results for class A and class B noisemodels," *IEEE Trans. Inf. Theory*, vol. 45, no. 4, pp. 1129–1149, May 1999.

[5] A. Spaulding and D. Middleton, "Optimum reception in an impulsive interference environment—Part I: Coherent detection," *IEEE Trans. Commun.*, vol. COM-25, no. 9, pp. 910–923, Sep. 1977.

[6] C. Tepedelenlioglu and P. Gao, "On diversity reception over fading channels with impulsive noise," *IEEE Trans. Veh. Technol.*, vol. 54, no. 6, pp. 2037–2047, Nov. 2005.

[7] T. Pander, "A suppression of an impulsive noise in ECG signal processing," in *Proc. IEEE Conf. EMBC*, 2004, vol. 1, pp. 596–599.

[8] R. C. Gonzalez and R. E. Woods, *Digital Image Processing*. Englewood Cliffs, NJ: Prentice-Hall, 2002.

[9] R. Chan, C. Ho, and M. Nikolova, "Salt-and-pepper noise removal by median-type noise detectors and detail-preserving regularization," *IEEE Trans. Image Process.*, vol. 14, no. 10, pp. 1479–1485, Oct. 2005.

[10] D. Ze-Feng, Y. Zhou-Ping, and X. You-Lun, "High probability impulse noise-removing algorithm based on mathematical morphology," *IEEE Signal Process. Lett.*, vol. 14, no. 1, pp. 31–34, Jan. 2007.

[11] W. Luo, "An efficient detail-preserving approach for removing impulse noise in images," *IEEE Signal Process. Lett.*, vol. 13, no. 7, pp. 413–416, Jul. 2006.

[12] C.-B. Wu, B.-D. Liu, and J.-F. Yang, "A fuzzy-based impulse noise detection and cancellation for real-time processing in video receivers," *IEEE Trans. Instrum. Meas.*, vol. 52, no. 3, pp. 780–784, Jun. 2003.

[13] I. Andreadis and G. Louverdis, "Real-time adaptive image impulse noise suppression," *IEEE Trans. Instrum. Meas.*, vol. 53, no. 3, pp. 798–806, Jun. 2004.

[14] S. Schulte, M. Nachtegael, V. De Witte, D. Van der Weken, and E. Kerre, "A fuzzy impulse noise detection and reduction method," *IEEE Trans. Image Process.*, vol. 15, no. 5, pp. 1153–1162, May 2006.

[15] E. Abreu, M. Lightstone, S. Mitra, and K. Arakawa, "A new efficient approach for the removal of impulse noise from highly corrupted images," *IEEE Trans. Image Process.*, vol. 5, no. 6, pp. 1012–1025, Jun. 1996.

[16] H. Eng and K. Ma, "Noise adaptive soft-switching median filter," *IEEE Trans. Image Process.*, vol. 10, no. 2, pp. 242–251, Feb. 2001.

[17] P. Ferreira and J. Vieira, "Stable DFT codes and frames," *IEEE Signal Process. Lett.*, vol. 10, no. 2, pp. 50–53, Feb. 2003.

[18] F. Marvasti, *Nonuniform Sampling: Theory and Practice*. Norwell, MA: Kluwer, 2001.

[19] P. Azmi and F. Marvasti, "A pseudo-inverse based iterative decoding method for DFT codes in erasure channels," *IEICE Trans. Commun.*, vol. 87, no. 10, pp. 3092–3095, 2004.

[20] R. E. Blahut, *Algebraic Codes for Data Transmission*. Cambridge, U.K.: Cambridge Univ. Press, 2003.

[21] F. Marvasti and M. Nafie, "Using FFT for error correction decoders," in *Proc. IEE Colloq. DSP Appl. Commun. Syst.*, 1993, p. 9.

[22] J. Wu and J. Shin, "Discrete cosine transform in error control coding," *IEEE Trans. Commun.*, vol. 43, no. 5, pp. 1857–1861, May 1995.

[23] P. Ferreira, "Stability issues in error control coding in the complex field, interpolation, and frame bounds," *IEEE Signal Process. Lett.*, vol. 7, no. 3, pp. 57–59, Mar. 2000.

[24] M. Skolnik, *Introduction to Radar Systems*. New York: McGraw-Hill, 2000.

[25] N. Nedev, S. McLaughlin, and D. Laurenson, "Estimating errors in transmission systems due to impulse noise," *Proc. Inst. Elect. Eng.—Commun.*, vol. 153, no. 5, pp. 651–656, Oct. 2006.

[26] D. Middleton, "Statistical-physical models of electromagnetic interference," *IEEE Trans. Electromagn. Compat.*, vol. 19, no. 3, pp. 106–127, Aug. 1977.

[27] M. Alamdari and M. Modarres-Hashemi, "An improved CFAR detector using wavelet shrinkage in multiple target environments," in *Proc. 9th Int. Symp. Signal Process. Appl.*, Sharjah, UAE, Feb. 12–15, 2007, pp. 1–4.

[28] S. Zahedpour, M. Ferdosizadeh, F. Marvasti, G. Mohimani, and M. Babaie-Zadeh, "A novel impulsive noise cancellation based on successive approximations," in *Proc. SampTa*, Thessaloniki, Greece, Jun. 2007.

[29] A. Amini, M. Babaie-Zadeh, and C. Jutten, "A fast method for sparse component analysis based on iterative detection–estimation," *AIP Conf. Proc.*, vol. 872, p. 123, 2006.

[30] A. Amini and F. Marvasti, "Reconstruction of multiband signals from noninvertible uniform and periodic nonuniform samples using an iterative method," in *Proc. SampTa*, Thessaloniki, Greece, Jun. 2007.

[31] A. Amini and F. Marvasti, "Convergence analysis of an iterative method for the reconstruction of multi-band signals from their uniform and periodic nonuniform samples," *Sampling Theory Signal Image Process.—Special Issue Nonuniform Sampling*, vol. 7, no. 2, May 2008. to be published.

[32] P. Azmi and F. Marvasti, "A novel decoding procedure for real field error control codes in the presentation of quantization noise," in *Proc. IEEE ICASSP*, 2003, vol. IV, pp. 265–268.

[33] K. Grochenig, "Acceleration of the frame algorithm," *IEEE Trans. Signal Process.*, vol. 41, no. 12, pp. 3331–3340, Dec. 1993.

[34] F. Marvasti, "Error concealment or correction of speech, image and video signals," United States Patent 6 601 206, Jul. 29, 2003.

Sina Zahedpour was born in Tehran, Iran, in 1984. He is currently working toward the B.Sc. degree in electrical engineering and communications at the Sharif University of Technology (SUT), Tehran.

Since 2006, he has been a Member of the Advanced Communication Research Institute, Department of Electrical Engineering, SUT, working on 1-D and 2-D signal denoising. His research interests include signal processing and information theory.

Soheil Feizi was born in Ardebil, Iran, in 1986. He is currently working toward the B.Sc. degree in electrical engineering, specializing in signal processing and communications at the Sharif University of Technology (SUT), Tehran, Iran.

Since 2006, he has been a Member of the Advanced Communication Research Institute, Department of Electrical Engineering, SUT, working with the Multimedia and Information Systems and Security Laboratories. His research interests include signal processing and wireless networks.

Mr. Feizi received the Best Student Award from the Department of Electrical Engineering, SUT.

Arash Amini was born in Arak, Iran, in 1982. He received the B.Sc. and M.Sc. degrees in electrical engineering and the B.Sc. degree in petroleum engineering from the Sharif University of Technology (SUT), Tehran, Iran, in 2005, 2006, and 2005 respectively, where he is currently working toward the Ph.D. degree.

He is also currently an active Member of the Advanced Communication Research Institute, Department of Electrical Engineering, SUT. His research interest is focused on signal processing, particularly different aspects of sampling.

Mahmoud Ferdosizadeh was born in Iran in 1979. He received the B.Sc. degree from the Amirkabir University of Technology, Tehran, Iran, and the M.Sc. degree in 2003 from the Sharif University of Technology (SUT), Tehran, where he is currently working toward the Ph.D. degree in communications and signal processing.

His research interests include MIMO OFDM and CDMA multiuser detection.

Farokh Marvasti received the B.Sc., M.Sc., and Ph.D. degrees in electrical engineering from Rensselaer Polytechnic Institute, Troy, NY, in 1970, 1971 and 1973, respectively.

From 1987 to 1991, he was an Associate Professor with the Illinois Institute of Technology, Chicago. From 1992 to 2003, he was an Instructor with the University of London, King's College, London, U.K. He was granted several research grants. He is currently a Professor in Sharif University of Technology, Tehran, Iran. His general research interests include signal processing, multiple access, MIMO techniques, and information theory.